

Formation of granular structures in trapped Bose-Einstein condensates under oscillatory excitations

V.I. Yukalov^{1,2*}, A.N. Novikov¹, and V.S. Bagnato²

¹*Bogolubov Laboratory of Theoretical Physics,
Joint Institute for Nuclear Research, Dubna 141980, Russia*

²*Instituto de Física de São Carlos, Universidade de São Paulo,
CP 369, 13560-970 São Carlos, São Paulo, Brazil*

Abstract

We present experimental observations and numerical simulations of nonequilibrium spatial structures in a trapped Bose-Einstein condensate subject to oscillatory perturbations. In experiment, first, there appear collective excitations, followed by quantum vortices. Increasing the amount of the injected energy leads to the formation of vortex tangles representing quantum turbulence. We study what happens after the regime of quantum turbulence, with increasing further the amount of injected energy. In such a strongly nonequilibrium Bose-condensed system of trapped atoms, vortices become destroyed and there develops a new kind of spatial structure exhibiting essentially heterogeneous spatial density. The structure reminds fog consisting of high-density droplets, or grains, surrounded by the regions of low density. The grains are randomly distributed in space, where they move. They live sufficiently long time to be treated as a type of metastable objects. Such structures have been observed in nonequilibrium trapped Bose gases of ^{87}Rb , subject to the action of alternating fields. Here we present experimental results and support them by numerical simulations. The granular, or fog structure is essentially different from the state of wave turbulence that develops after increasing further the amount of injected energy.

*Corresponding author (V.I. Yukalov):

E-mail: yukalov@theor.jinr.ru

1 Granular structure characteristics

A granular structure is understood as an inhomogeneous mixture of sufficiently large dense formations, called grains, surrounded by a much less dense phase, such as gas. That is, a granular structure does not constitute a single phase of matter, but has the properties of two or more intermixed phases. Such granular materials are ubiquitous in nature, usually being a mixture of solid formations separated by gaseous phase [1–3].

In the present paper, we consider a mixture enjoying similar properties, though being very different from the usual granular materials. It is also an inhomogeneous composition of two phases, more dense and essentially less dense one. Although the more dense phase is not solid. The main difference of the mixture we shall consider is that both phases, the dense and rarified one, are formed by the same type of atoms. Such a mixture can be created in a cloud of trapped Bose-condensed atoms and in optical lattices. Before describing the concrete case of trapped atoms, let us emphasize the general features of the granular mixture that we will be considering in what follows. There are five main properties characterizing such a granular structure.

(i) The structure is composed of the same type of atoms that form two or more different phases. As a whole, the system is not equilibrium, but it has to be in a locally equilibrium state in order that it could be possible to speak of different phases forming the mixture. This requirement distinguishes the mixture, we shall consider, from the usual granular materials, such as sand, coal, rice, coffee, or corn flakes, whose grains are formed of different atoms as compared to the surrounding air. To be in local equilibrium the typical grain lifetime t_g has to be much larger than the local equilibration time t_{loc} .

(ii) The spatial distribution of grains at a snapshot is random. They constitute no ordered structure, such as domains, stripes or other patterns.

(iii) The spatial locations of grains in different experiments is also random, so that there is no repeating spatial structure, but they are randomly distributed.

(iv) The typical linear size of grains, l_g , is mesoscopic, being between the scattering length a_s of atoms composing a grain and the total system size L , so that $a_s \ll l_g \ll L$.

(v) The grains are of multiscale nature, having the sizes in a dense interval $[l_{min}, l_{max}]$ and possessing different shapes. This means that the mentioned typical size l_g is not just a single fixed quantity, but an average typical quantity from an interval $[l_{min}, l_{max}]$.

These features make it rather difficult to describe such a granular mixture composed of grains that are random in shapes, sizes, and in spatial distribution. In addition, to create a granular mixture of the considered type it is, generally, necessary to strongly perturb the atomic system, moving it far from equilibrium.

2 Perturbing trapped condensate

In this section, we delineate the general sequence of states through which the system of trapped condensed atoms passes in the process of their excitation by an external field, when gradually increasing its strength and time of action. A concrete experiment with ^{87}Rb will be described in Sec. 3 and numerical simulations discussed in Sec. 4.

Trapped Bose atoms in equilibrium at low temperatures form Bose-Einstein condensate in the ground state. The condensate cloud in a trap enjoys approximately Thomas-Fermi

shape, with well known properties described in the books [4–7] and reviews [8–18]. In order to strongly perturb the condensate, it is necessary to impose external perturbations transferring the condensate from its ground state to excited states. There are two main ways of imposing such external perturbations.

One possibility is to add to the static trapping potential $U(\mathbf{r})$ an alternating potential $V(\mathbf{r}, t)$, so that the total trap potential becomes

$$U(\mathbf{r}, t) = U(\mathbf{r}) + V(\mathbf{r}, t) . \quad (1)$$

Another way is to modulate the scattering length $a_s(t)$ by means of Feshbach resonance techniques. Both these ways can be used for strongly disturbing Bose-Einstein condensates.

Suppose trapped Bose atoms have been cooled down to very low temperatures, when practically all of them pile down to a Bose-condensed state. And let us apply an external modulating perturbation by one of the methods mentioned above. First, at weak perturbation, there appear elementary collective excitations that are small deviations from the ground state. Weak perturbations also can generate large deviations from the ground state, provided that the modulation frequency is in resonance with one of the transition frequencies between topological coherent modes [19, 20]. The latter are defined as the eigenfunctions of the nonlinear stationary Schrödinger equation

$$\left[-\frac{\nabla^2}{2m} + U(\mathbf{r}) + N\Phi_0|\varphi_n(\mathbf{r})|^2 \right] \varphi_n(\mathbf{r}) = E_n\varphi_n(\mathbf{r}) , \quad (2)$$

where N is the number of condensed atoms, assumed to be close to the total number of atoms, and

$$\Phi_0 \equiv 4\pi \frac{a_s}{m} \quad (3)$$

is the atomic interaction strength, in which a_s is a scattering length assumed to be positive. The modes are termed topological, since they have different number of zeroes, thus, topologically different atomic density. They are coherent, being formed by condensed atoms characterized by a coherent state.

In the above equations, the Planck constant is set to unity. While we shall restore it below for the clarity of numerical estimates.

The known particular example of the topological modes are quantum vortices. If the external perturbation rotates the atomic cloud, acting as a spoon, then vortices appear being aligned along the imposed axis of rotation. But when the trap modulation does not prescribe a fixed rotation axis, then vortices and antivortices arise in pairs or in larger groups [8, 19]. The explicit experimental demonstration for the appearance of clusters of vortices and antivortices was done in Ref. [21].

Increasing the strength of the trap modulation generates a variety of coherent modes, needing no resonance conditions because of the power broadening effect [22]. Among these numerous coherent modes, the basic vortex, with the winding number one, is the most energetically stable. For a trap with a transverse, ω_\perp , and longitudinal, ω_z , frequencies, the vortex energy can be written [7] as

$$\omega_{vor} = \frac{0.9\omega_\perp}{(\nu g)^{2/5}} \ln(0.8\nu g) , \quad (4)$$

where the notation is used for the trap aspect ratio

$$\nu \equiv \frac{\omega_z}{\omega_\perp} = \left(\frac{l_\perp}{l_z} \right)^2 \quad (5)$$

and for the effective coupling parameter

$$g \equiv 4\pi N \frac{a_s}{l_\perp} , \quad (6)$$

with l_\perp and l_z being the transverse and longitudinal oscillator lengths, respectively. Due to the large number of atoms N , the effective coupling parameter is large, $g \gg 1$. As is seen, the basic vortex energy diminishes with the increase of g . At the same time, the transition frequencies of other modes, hence their energies, can be shown [19, 22] to increase as

$$\omega_{mn} \propto (\nu g)^{2/5} \quad (g \gg 1) . \quad (7)$$

This makes the basic vortex the most energetically stable mode.

When the trap aspect ratio is not too small, the trap can house many vortices. The latter are created due to dynamic instability arising in the moving fluid [23–30].

Increasing the strength of the pumping, without imposing any rotation axis, produces a tangle of vortices, which makes the trapped atomic cloud turbulent [31–35]. Increasing further either the amplitude of the pumping field or the pumping time leads to the appearance of different structures, such as the granulated condensate state.

The energy, injected into the trap by means of an external perturbation modulating the trapping potential, can be written as

$$E_{inj} = \int \rho(\mathbf{r}, t) \left| \frac{\partial V(\mathbf{r}, t)}{\partial t} \right| d\mathbf{r} dt , \quad (8)$$

where $\rho(\mathbf{r}, t)$ is atomic density. In the case of a periodic in time alternating field $V(\mathbf{r}, t) \sim A \cos(\omega t)$, the energy, injected during the modulation time t , takes the form $E_{inj} \approx \omega t$. This makes it possible to represent the crossover lines between different regimes as the relation

$$A \sim \frac{\pi E_{inj}}{2\omega t} \quad (9)$$

between the amplitude A of the pumping field and the pumping time t .

The system properties also depend on pair atomic interactions that are conveniently characterized by the gas parameter

$$\gamma \equiv \rho^{1/3} a_s = \frac{a_s}{a} , \quad (10)$$

which is usually small for trapped atoms, although can be varied in a wide range by means of the Feshbach resonance techniques. Despite the gas parameter γ can be small, but the effective coupling parameter g is usually large because of the large number of atoms in a trap.

An important quantity, showing whether atoms are in local equilibrium, is the local equilibration time

$$t_{loc} \equiv \frac{m}{\hbar \rho a_s} = 4\pi \frac{m \xi^2}{\hbar} ,$$

where $\xi \equiv 1/\sqrt{4\pi\rho a_s}$ is the coherence length. A perturbed cloud of trapped atoms, as a whole, can be strongly nonequilibrium, while, at the same time, be locally equilibrium. This happens in the situation, when the modulation period $t_{mod} \equiv 2\pi/\omega$ of the alternating modulating field, with frequency ω , is much longer than the local equilibration time t_{loc} .

3 Modulation of trapping potential for ^{87}Rb

In experiments, the granular condensate structures are created for trapped ^{87}Rb by modulating the trap with a time alternating potential.

The cloud of ^{87}Rb atoms, of mass $m = 1.443 \times 10^{-22}$ g and scattering length $a_s = 0.557 \times 10^{-6}$ cm, is cooled down to temperatures much lower than the Bose-Einstein condensation temperature $T_c = 276$ nK, so that the great majority of all $N = 2 \times 10^5$ atoms are condensed, with the condensate fraction being $n_0 = 0.7$.

The trap is of cylindrical shape, with the frequencies $\omega_{\perp} = 2\pi \times 210$ Hz and $\omega_z = 2\pi \times 23$ Hz, which corresponds to the oscillator lengths $l_{\perp} = 0.74 \times 10^{-4}$ cm and $l_z = 2.25 \times 10^{-4}$ cm. Respectively, the trap aspect ratio is $\nu = 0.11$. The effective coupling parameter is $g = 1.96 \times 10^4$.

The atomic cloud is characterized by the sizes that can be estimated as $r_{\perp} = 2.27 \times 10^{-4}$ cm, $z_0 = 1.47 \times 10^{-3}$ cm, which makes it possible to find the effective atomic density $\rho = 0.43 \times 10^{15}$ cm $^{-3}$ and the mean interatomic distance $a = 1.32 \times 10^{-5}$ cm. The gas parameter is small, $\gamma \sim 1.4 \times 10^{-3}$, while the effective coupling is large, $g = 1.96 \times 10^4$.

The trap potential is modulated by an additional alternating potential $V(\mathbf{r}, t)$ (see [21, 35, 36]) oscillating with the frequency $\omega = 1.26 \times 10^3$ s $^{-1}$, which corresponds to the modulation period $t_{mod} = 0.5 \times 10^{-2}$ s. The total modulation time t_{ext} is varied between 0.02 s and 0.1 s. The local equilibration time is $t_{loc} = 0.57 \times 10^{-3}$ s. Thus, the relations between the characteristic times is

$$t_{loc} \ll t_{mod} \ll t_{ext} ,$$

which means that the system is locally equilibrium, although as a whole it is strongly nonequilibrium.

Because of the high atomic density inside the trap, the *in situ* observation is impossible. Absorption pictures are taken in the time-of-flight setup, after the times t_{tof} between 0.015 s and 0.023 s. The turbulent and granular structures, consequently created by increasing the excitation time, are displayed in Fig. 1. The final stage, corresponding to the granular state, is shown in details in Fig. 2. Since the image is obtained through the absorption by a three-dimensional expanding cloud, the contrast between the grains and rarified gas surrounding them is not very sharp. Restoring the characteristic linear size of grains before the free expansion, we get $l_g \approx 3 \times 10^{-5}$ cm. The relation between the characteristic lengths is

$$a_s \ll a \sim \xi \sim l_g \ll l_z .$$

This shows that the grains are of mesoscopic size, being in between the scattering length and the linear system size. At the same time, the grain linear size is close or slightly larger than the coherence length, which suggests that each grain represents a coherent formation.

The excitation of strongly nonuniform states can also be realized by modulating the scattering length [37, 38]. Generally, long modulation times or large exciting amplitudes

generate the cloud evolution from the appearance of separate vortices to tangled vortex configurations, typical of quantum turbulence, after which the granular state arises.

The experimental phase diagram on the amplitude-time $A - t$ plane is described in Refs. [33,34], where it is shown that with increasing the injected energy, that is proportional to the product At , the system passes through the following states: *regular superfluid* slightly perturbed by a random weak external field, *vortex superfluid* with several vortices, *turbulent superfluid* formed by a tangle of many vortices, and *granular state* with condensate droplets surrounded by a gas of low density.

4 Numerical simulations for ^{87}Rb experiment

In order to better understand the properties of the granular state, we have accomplished numerical simulations for exactly the same setup and parameters as in experiment [33–35] with ^{87}Rb .

The simulation is based on the nonlinear Schrödinger equation, with the parameters corresponding to the experiments [33–35]. The same alternating potential modulating the trap as in these experiments is used. The amount of the energy pumped into the trap, as is illustrated in Eq. (8), is proportional to the amplitude of the modulating potential and to the pumping time, approximately through the product of these. Increasing E_{inj} , we in turn observe first, a slightly nonequilibrium regular Bose-condensed atomic cloud, then the appearance of separate vortices. After the number of vortices reaches about 25, the regime of quantum vortex turbulence develops corresponding to the random vortex tangle. These regimes of the *regular superfluid*, *vortex state*, and *vortex turbulence* have been thoroughly described in our previous papers [33–35]. Therefore here we pay the main attention to the granular state that arises after the regime of vortex turbulence.

The increase of the injected energy E_{inj} leads, after the vortex turbulence, to the appearance of the granular state, when there are no vortices, but the system decomposes into a number of dense grains, or droplets, inside a rarified surrounding. The density of the grains is up to 100 times larger than that of their surrounding. The order-parameter phase is practically the same inside each grain, confirming that these grains are the droplets of Bose-condensed atoms. But the phases inside different grains can be different. The grains differ from vortices by the absence of their vorticity. A typical granular structure is illustrated in Fig. 3.

The sizes of the grains vary in the range between 1×10^{-5} cm to 3×10^{-5} cm. Although they are not spherical, but their linear sizes in the radial and longitudinal directions are close to each other.

After the granular state has been created, we have analyzed its stability by switching off the perturbing potential and observing the spatio-temporal behavior of the system. The grains can move in space, slightly changing their shapes, sometimes fusing with each other, but survive during the period of time of order 10^{-2} s. The grain lifetime for ^{87}Rb is in agreement with the estimate $t_g \sim (\xi/a_s)t_{loc}$ for the heterophase lifetime [39] giving for ^{87}Rb the same order of 10^{-2} s. The grain lifetime is much longer than the local-equilibration time $t_{loc} \sim 10^{-4}$ s, which proves that the grains can be treated as quasi-equilibrium formations. The spatio-temporal behavior of the grains is demonstrated in the sequence of the transverse cross-sections in Fig. 4.

In each realization, either numerical or experimental, the spatial distribution of grains is random and does not repeat from one realization to another. The regime corresponding to this random granular state can be termed *grain turbulence*. Since the system in this state consists of two types of regions of drastically different density, hundreds of time differing from each other, such a state is an example of a *heterogeneous*, or *heterophase*, state. Therefore the grain turbulence is a particular case of heterophase turbulence [40].

Finally, increasing the amount of injected energy, after the regime of the grain turbulence, another state develops, consisting of uniformly distributed in space weak waves, whose density is only about 3 times larger than that of their surrounding. The typical linear sizes of separate waves are between 0.3×10^{-4} cm to 0.8×10^{-4} cm. The phases inside the waves as well as between them are random.

This wave regime corresponds to the so-called *wave turbulence*, or *weak turbulence*. The latter is principally different from the regime of *grain turbulence*. The regime of weak turbulence is demonstrated in Fig. 5 as the sequence of density snapshots. Our simulations show that the regimes of grain turbulence and wave turbulence are clearly distinguished by the following main features:

(i) The waves are weak, having the amplitudes only about 3 times larger than the most rarified parts of the system, while the grains are dense formations whose density is up to 100 times larger than that of their surrounding.

(ii) The phase inside each wave is rather random, while the phase inside a grain is practically constant. This implies that the wave turbulence, actually, corresponds to the situation when the condensate is destroyed in the whole system, while grain turbulence describes the intermediate case, where there exist coherent Bose condensate germs, or droplets, inside a rarified normal phase.

(iii) In the regime of wave turbulence, the system kinetic energy is more than 100 times larger than the interaction energy, while under grain turbulence the former is only about five times larger than the latter.

In this way, wave turbulence, we reproduce in numerical simulations, completely satisfies the commonly accepted basic features of this regime [41]. And the grain turbulence corresponds to the intermediate regime of random turbulent cells in the Kibble-Zurek [42, 43] picture of transition between the vortex turbulence and normal turbulent state. It is possible to show [44] that there exists a mapping between the states of an atomic bosonic cloud, subject to an alternating trap modulation, and the states of an atomic system in a random spatial external potential [45]. According to this mapping, grain turbulence corresponds to a disordered Bose system and the wave turbulence, to the normal state with destroyed Bose condensate.

5 Conclusion

We have presented experimental evidence for the formation of granulated Bose-Einstein condensate, consisting of dense condensate droplets immersed into the surrounding rarified gas. The density of the grains can be hundred times larger than that of the surrounding gas. Such granulated Bose condensates have been observed in nonequilibrium trapped Bose gases of ^{87}Rb , under alternating trap modulation.

Numerical simulations, based on the nonlinear Schrödinger equation, with the parameters exactly corresponding to the experiments with ^{87}Rb , reproduce well all the stages of the condensate excitation by means of the trapping potential alternation. Increasing the amount of energy, injected into the system by the trap modulation, we observe in turn the following states: slightly perturbed *regular Bose-Einstein condensate*, *vortex state*, with a few vortices and antivortices, *vortex turbulence* formed by a random tangle of quantum vortices, *grain turbulence* represented by randomly distributed grains of dense Bose-condensate droplets inside a very rarified gas, and *wave turbulence* consisting of the random waves of small amplitude, where spatial coherence is destroyed.

Our numerical simulations confirm that the granular state can be considered as a metastable state, since the lifetime of the coherent grains is much longer than the local equilibration time. The existence and properties of granulated structures essentially depend on the system parameters.

In a recent experiment performed in the laboratory of R. Hulet, using ^7Li and modulation of interaction, it seems there has also been observed the formation of granular structure. This is currently under investigation and will be the topic of a future publication.

Acknowledgement

Financial support from FAPESP and CNPQ (Brazil) is appreciated. Two of the authors (A.N.N. and V.I.Y.) acknowledge financial support from the Russian Foundation for Basic Research. One of the authors (V.I.Y.) is grateful for discussions to E.P. Yukalova.

References

- [1] Bagnold R A 1941 *The Physics of Blown Sand and Desert Dunes* (London: Methuen)
- [2] Duran J 1999 *Sands, Powders, and Grains: An Introduction to the Physics of Granular Materials* (New York: Springer)
- [3] Pudasaini S P and Hutter K 2007 *Avalanche Dynamics: Dynamics of Rapid Flows of Dense Granular Avalanches* (Berlin: Springer)
- [4] Pitaevskii L and Stringari S 2003 *Bose-Einstein Condensation* (Oxford: Clarendon)
- [5] Lieb E H, Seiringer R, Solovej J P and Yngvason J 2005 *The Mathematics of the Bose Gas and Its Condensation* (Basel: Birkhauser)
- [6] Letokhov V 2007 *Laser Control of Atoms and Molecules* (New York: Oxford University)
- [7] Pethick C J and Smith H 2008 *Bose-Einstein Condensation in Dilute Gases* (Cambridge: Cambridge University)
- [8] Courteille P W, Bagnato V S and Yukalov V I 2001 *Laser Phys.* **11** 659
- [9] Andersen J O 2004 *Rev. Mod. Phys.* **76** 599
- [10] Yukalov V I 2004 *Laser Phys. Lett.* **1** 435
- [11] Bongs K and Sengstock K 2004 *Rep. Prog. Phys.* **67** 907
- [12] Yukalov V I and Girardeau M D 2005 *Laser Phys. Lett.* **2** 375
- [13] Posazhennikova A 2006 *Rev. Mod. Phys.* **78** 1111
- [14] Yukalov V I 2007 *Laser Phys. Lett.* **4** 632
- [15] Proukakis N P and Jackson B 2008 *J. Phys. B* **41** 203002
- [16] Yurovsky V A, Olshanii M and Weiss D S 2008 *Adv. At. Mol. Opt. Phys.* **55** 61
- [17] Yukalov V I 2009 *Laser Phys.* **19** 1
- [18] Yukalov V I 2011 *Phys. Part. Nucl.* **42** 460
- [19] Yukalov V I, Yukalova E P and Bagnato V S 1997 *Phys. Rev. A* **56** 4845
- [20] Yukalov V I, Yukalova E P and Bagnato V S 2000 *Laser Phys.* **10** 26
- [21] Seman J A, Henn E A L, Haque M, Shiozaki R F, Ramos E R F, Caracanhas M, Castilho P, Castelo Branco C, Tavares P E S, Poveda-Cuevas F J, Roati G, Magalhães K M F and Bagnato V S 2010 *Phys. Rev. A* **82** 033616
- [22] Yukalov V I, Yukalova E P and Bagnato V S 2002 *Phys. Rev. A* **66** 043602
- [23] Yukalov V I 1980 *Acta Phys. Pol. A* **57** 295

- [24] Dutton Z, Budde M, Slowe C and Hau L V 2001 *Science* **293** 663
- [25] Yukalov V I and Yukalova E P 2004 *Laser Phys. Lett.* **1** 50
- [26] Ruostekoski J and Dutton Z 2005 *Phys. Rev. A* **72** 063626
- [27] Shomroni I, Lahoud E, Levy S and Steinhauer J 2009 *Nature Phys.* **5** 193
- [28] Ma M, Carretero-Gonzalez R, Kevrekidis P G, Frantzeskakis D J and Malomed B A 2010 *Phys. Rev. A* **82** 023621
- [29] Ishiro S, Tsubota M and Takeuchi H 2011 *Phys. Rev. A* **83** 063602
- [30] Simula T P 2011 *Phys. Rev. A* **84** 021603
- [31] Henn E A L, Seman J A, Roati G, Magalhães K M F and Bagnato V S 2009 *Phys. Rev. Lett.* **103** 045301
- [32] Seman J A, Shiozaki R F, Poveda-Cuevas F J, Henn E A L, Magalhães K M F, Roati G, Telles G D and Bagnato V S 2011 *J. Phys. Conf. Ser.* **264** 012004
- [33] Shiozaki R F, Telles G D, Yukalov V I and Bagnato V S 2011 *Laser Phys. Lett.* **8** 393
- [34] Seman J A, Henn E A L, Shiozaki R F, Roati G, Poveda-Cuevas F J, Magalhães K M F, Yukalov V I, Tsubota M, Kobayashi M, Kasamatsu K and Bagnato V S 2011 *Laser Phys. Lett.* **8** 691
- [35] Bagnato V S and Yukalov V I 2013 *Prog. Opt. Sci. Photon.* **1** 377
- [36] Henn E A L, Seman J A, Ramos E R F, Caracanhas M, Castilho P, Olimpio E P, Roati G, Magalhães D V, Magalhães K M F and Bagnato V S 2009 *Phys. Rev. A* **79** 043618
- [37] Ramos E R F, Henn E A L, Seman J A, Caracanhas M A, Magalhães K M F, Helmerson K, Yukalov V I and Bagnato V S 2008 *Phys. Rev. A* **78** 063412
- [38] Pollack S E, Dries D, Hulet R G, Magalhães K M F, Henn E A L, Ramos E R F, Caracanhas M A and Bagnato V S 2010 *Phys. Rev. A* **81** 053627
- [39] Yukalov V I 1991 *Phys. Rep.* **208** 395
- [40] Yukalov V I 2003 *Int. J. Mod. Phys.* **17** 2333
- [41] Zakharov V E, Lvov V S and Falkovich G E 1992 *Kolmogorov Spectra of Turbulence - Wave Turbulence* (Berlin: Springer)
- [42] Kibble T W 1976 *J. Phys. A* **9** 1387
- [43] Zurek W H 1996 *Phys. Rep.* **276** 177
- [44] Yukalov V I, Yukalova E P and Bagnato V S 2009 *Laser Phys.* **19** 686
- [45] Yukalov V I and Graham R 2007 *Phys. Rev. A* **75** 023619

Figure Captions

Fig. 1. Image of the full sample observed by absorption in experiments with ^{87}Rb . The turbulent cloud of vortices (top) demonstrates the random vortex tangle, while the granular state (bottom) consists of the domains of very different atomic density, reminding droplets. The granulation appears when perturbing the system for long time, after passing through the stage of vortex turbulence.

Fig. 2. Details of the observed absorption image of a granulated atomic superfluid of ^{87}Rb . The domains of high density of a variety of sizes and shapes are seen.

Fig. 3. The granular structure of ^{87}Rb realized in numerical modeling. The grains (droplets) are clearly seen in the density snapshots.

Fig. 4. Spatio-temporal behavior of the grains illustrated by numerical simulations. Each column represents the sequence of transverse cross-sections of the atomic cloud at different relaxation times $\tau = 0; 1, 5; 3$ and 5 ms (from left to right), after the perturbing potential is switched off. The granular structure becomes blurred during the time, but still well observable after 5 ms.

Fig. 5. Transverse cross-sections of the ^{87}Rb atomic cloud, corresponding to the regime of wave turbulence, as found in numerical simulations.

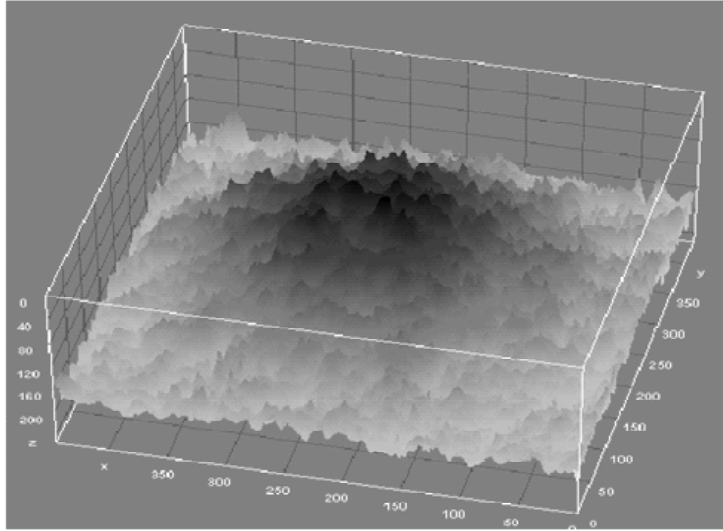
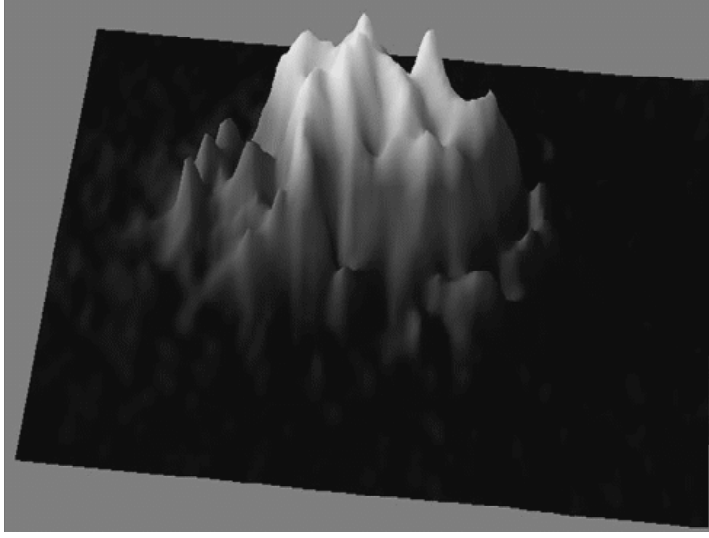


Figure 1: Image of the full sample observed by absorption in experiments with ^{87}Rb . The turbulent cloud of vortices (top) demonstrates the random vortex tangle, while the granular state (bottom) consists of the domains of very different atomic density, reminding droplets. The granulation appears when perturbing the system for long time, after passing through the stage of vortex turbulence.

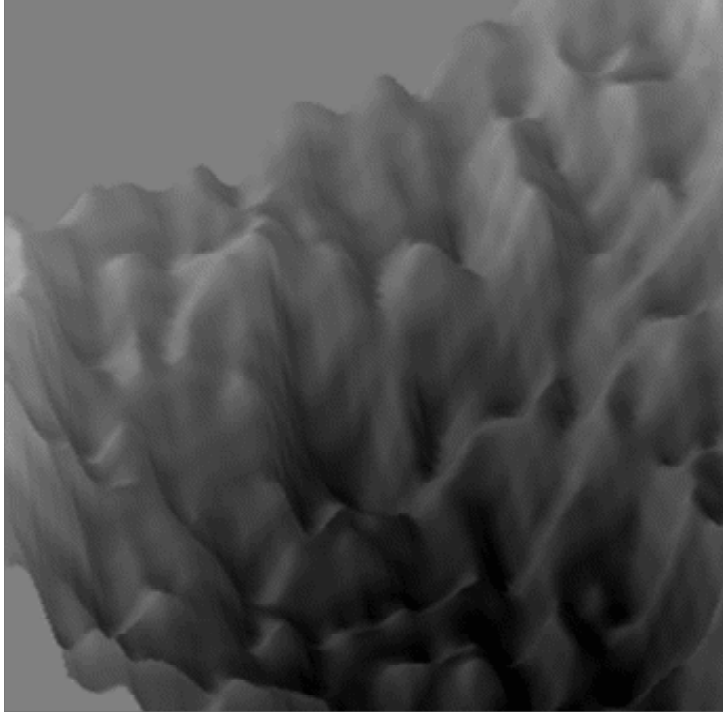


Figure 2: Details of the observed absorption image of a granulated atomic superfluid of ^{87}Rb . The domains of high density of a variety of sizes and shapes are seen.

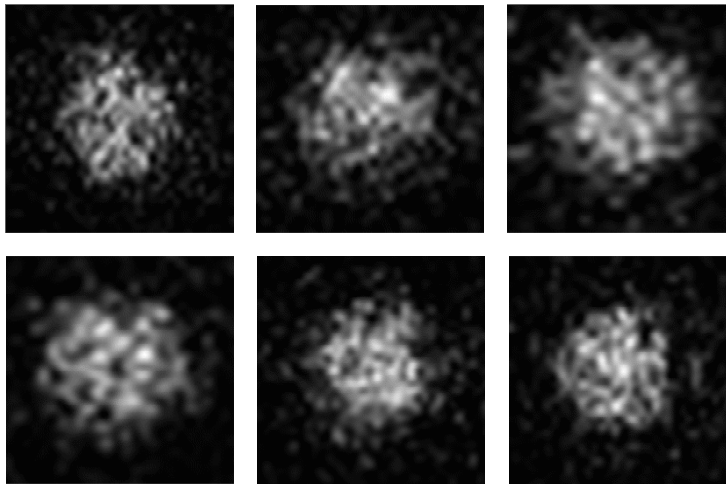


Figure 3: The granular structure of ^{87}Rb realized in numerical modeling. The grains (droplets) are clearly seen in the density snapshots.

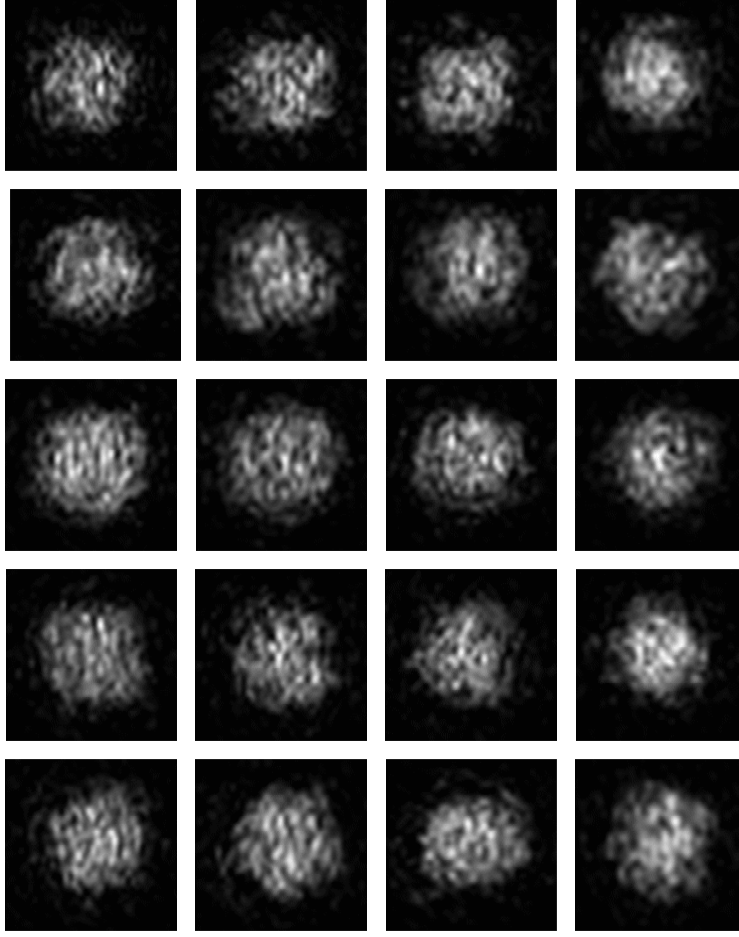


Figure 4: Spatio-temporal behavior of the grains illustrated by numerical simulations. Each column represents the sequence of transverse cross-sections of the atomic cloud at different relaxation times $\tau = 0; 1, 5; 3$ and 5 ms (from left to right), after the perturbing potential is switched off. The granular structure becomes blurred during the time, but still well observable after 5 ms.

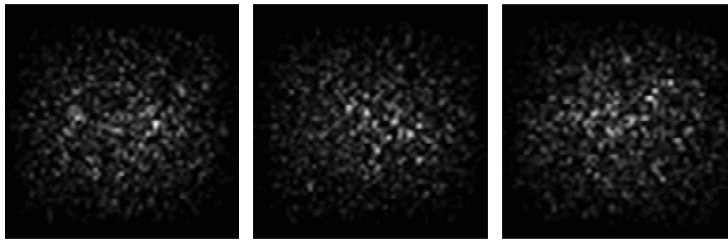


Figure 5: Transverse cross-sections of the ^{87}Rb atomic cloud, corresponding to the regime of wave turbulence, as found in numerical simulations.